INSTITUTE OF PHYSICS PUBLISHING JOURNAL OF PHYSICS: CONDENSED MATTER

J. Phys.: Condens. Matter **17** (2005) S3469–S3479 doi:10.1088/0953-8984/17/45/036

Interface–solvent effects during colloidal phase transitions

Sylvie Roke[1,6], Johan Buitenhuis[2], J C van Miltenburg[3], Mischa Bonn[1,4] and Alfons van Blaaderen[5]

[1] Leiden Institute of Chemistry, Leiden University, PO Box 9502, 2300 RA Leiden, The Netherlands
[2] Research Center Juelich, Institute for Solid State Research, Soft Matter, 52425 Juelich, Germany
[3] Chemical Thermodynamics Group, Debye Institute, Utrecht University, PO Box 80051, 3508 TB Utrecht, The Netherlands
[4] FOM-Institute for Atomic and Molecular Physics, Kruislaan 407, 1098 SJ Amsterdam, The Netherlands
[5] Soft Condensed Matter, Debye Institute, Utrecht University, PO Box 80000, 3508 TA Utrecht, The Netherlands

E-mail: roke@mf.mpg.de

Received 5 October 2005
Published 28 October 2005
Online at stacks.iop.org/JPhysCM/17/S3469

Abstract

We have compared calorimetric measurements with the nonlinear optical technique vibrational sum frequency scattering to investigate interface–solvent effects in colloidal gelation transitions. This allows us to explain the difference in gelation behaviour between dispersions of stearyl-coated silica particles in n-hexadecane and benzene or toluene. In n-hexadecane dispersions, an anomalous heat effect is observed, due to the formation of an ordered interface layer (that is not confined to the first monolayer and is composed of $\sim 1/3$ surface crafted chains and $\sim 2/3$ solvent molecules). For solvents that cannot interdigitate with the surface chains this transition does not occur and consequently no heat effect is observed.

1. Introduction

Colloidal dispersions are found in nature in many forms and are applied in many branches of technology [1–5]. The stability of these dispersions depends on the particle interaction potential. Often this potential reflects (unwanted) attraction between the particles and consequently a repulsion needs to be introduced to keep the dispersion stable. In aqueous solutions, this can be achieved by creating a surface charge layer on the particles. In non-aqueous apolar solvent, repulsion can be introduced by steric stabilization of the particles. This is achieved by functionalizing the particles with apolar surface chains. A well-known example

[6] Present address: Max-Planck Institute for Metals Research, Heisenbergstraße 3, 70569 Stuttgart, Germany.

consists of silica particles with octadecyl chains crafted at the surface [6]. These particles are stable in many apolar solvents and are often considered as the colloidal equivalent of an ideal gas. However, it was found that with certain solvents the dispersion can become unstable as the temperature is lowered and phase separates [7–14], or forms a gel. The instability could be induced as well by changing the pressure [15]. The gelation was explained as a consequence of percolation [16], as a dynamic instability [17], and as a frustrated gas–solid transition [18], and it was suggested that the interface–solvent interaction plays a key role in the phase transition [15].

As all thermodynamic, linear scattering and microscopy techniques cannot reveal molecular details directly it is not possible to obtain conclusive evidence regarding the role of the interface in these transitions. This has become possible only very recently with the development of second-order nonlinear optical scattering techniques that can provide information selectively from the interface region of the particles in a solution [19–23]. More specifically, the recent development of vibrational sum frequency scattering [24–26] allows direct access to the molecular structure of the interface, since vibrational modes at the interface are probed directly. In a vibrational sum frequency scattering experiment, interface vibrational modes are resonantly excited by infrared photons. The resulting polarization is upconverted with visible photons and a field with the sum of the frequencies is emitted. Due to the second-order nature of this process, it is interface specific. As the particles are much smaller than the exciting laser beams the sum frequency light is scattered from the particle interfaces and is collected at a certain scattering angle. While the frequency content of the resulting spectrum is determined by the average molecular interface structure, the intensity distribution is determined by the particle size and shape. As we are only interested in the interfacial changes we measure at a fixed angle.

In a previous study we have demonstrated that it is possible to observe the molecular changes that occur during a colloidal gelation transition. Also we found that surface effects may modify the speed of ageing [26]. In the study presented here we focus on the influence of solvents on the molecular arrangement of surface groups and how this affects the interface during gelation. To this end we will compare calorimetric data with sum frequency scattering experiments.

2. Experimental details

The bare silica dispersions denoted as samples 1, 2, and 3 in table 1 were synthesized according to Stöber's [27] method. Sample 4 was grown with silica from core particles (seeded growth), using small Ludox particles (from DuPont) as starting material [28]. The bare silica dispersions were then coated with stearyl alcohol according to [6]. The dispersions in cyclohexane were dried under a dry nitrogen flow at 373 K and redispersed in n-hexadecane (99%, Janssen Chimica, Sigma Aldrich), n-hexadecane-d_{34} (98 at.% D, Aldrich), benzene-d_6 (99 at.% D, Sigma Aldrich) or toluene (>99%, Baker AR). All dispersions were prepared on a weight basis. The volume fractions were calculated assuming additivity of volumes, using a density for stearyl silica of 1.75 g ml^{-1} as determined for sample 1 in [9].

Table 1 summarizes the particle characteristics as determined from dynamic light scattering (DLS) and transmission electron microscopy (TEM). The relative width ($\Delta\sigma$) of the distribution is defined as the standard deviation of the radius divided by the average radius (σ). Calorimetric measurements were performed on a differential scanning calorimeter DSC III from Setaram, with a detection limit of 0.2 J g^{-1}. The temperature of the gelation transition in the dispersion was determined by performing a temperature scan and observing at which temperature the gel starts to flow. If small gas bubbles ($\sim$0.1 mm) did not rise any more, the

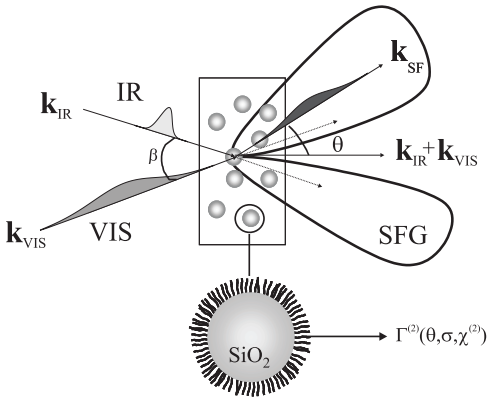

Figure 1. Schematic sketch of the sum frequency scattering experiment. The scattered sum frequency light is recorded in one direction. The magnitude and spectral shape of the scattered field is determined by the molecular configuration at the interface which is contained in the second-order nonlinear susceptibility ($\chi^{(2)}$). For a particular geometry (defined by the **k** vectors and detector angle) and particle size (σ), $\chi^{(2)}$ can be determined from the effective particle susceptibility $\mathbf{\Gamma}^{(2)}$.

Table 1. Characterization of the particles.

Particles[a]	σ_{DLS} (nm)	σ_{TEM} (nm)	$\Delta\sigma$
Sample 1 (SJ9)	36	30	0.15
Sample 2 (AB80)	85	73	0.06
Sample 3 (DB284)	130	123	0.05
Sample 4 (SLC4)	30	20	0.14

[a] The particle code as used in previous literature is given in parentheses.

dispersions were classified as gel. Also, the temperature of the bending point in a turbidity–temperature scan using spectrophotometry was obtained.

The sum frequency generation (SFG) experiments were performed using 7 μJ (120 fs) infrared (IR) pulses (repetition rate 1 kHz, FWHM bandwidth of $\sim$180 cm^{-1}) centred around 2900 cm^{-1} and 3 μJ, 800 nm visible (VIS) pulses with a 7 cm^{-1} bandwidth. A schematic representation of the experimental geometry can be found in figure 1. The selectively polarized IR and VIS pulses were incident under a relative angle of 15° (β) and focused down to a $\sim$0.4 mm beam waist. The scattered light was collimated with a lens (with an angular acceptance of 17°), polarization selected and dispersed onto an intensified charge coupled device (CCD) camera [29, 30]. The sample cell consisted of a cuvette (Hellma GmbH) with a volume of 280 μl and a path length of 1 mm. The scattering angle θ (as measured in air) was 51°. For temperature-dependent scattering and turbidity measurements, the sample temperature was raised by resistively heating the sample holder, resulting in a constant heating rate of typically 2.9 K min^{-1}. The temperature was measured with a small thermocouple placed in the cell $\sim$1 mm away from the laser focus.

3. Solvent dependence

3.1. Calorimetry

To investigate gelation in various solvents we have recorded the volume fraction φ at which a gel can be formed in n-hexadecane, toluene or benzene. For the dispersion of sample 1 in n-hexadecane we find gel formation at $\varphi \approx 9.8$ and Jansen [9] observed gel formation for sample

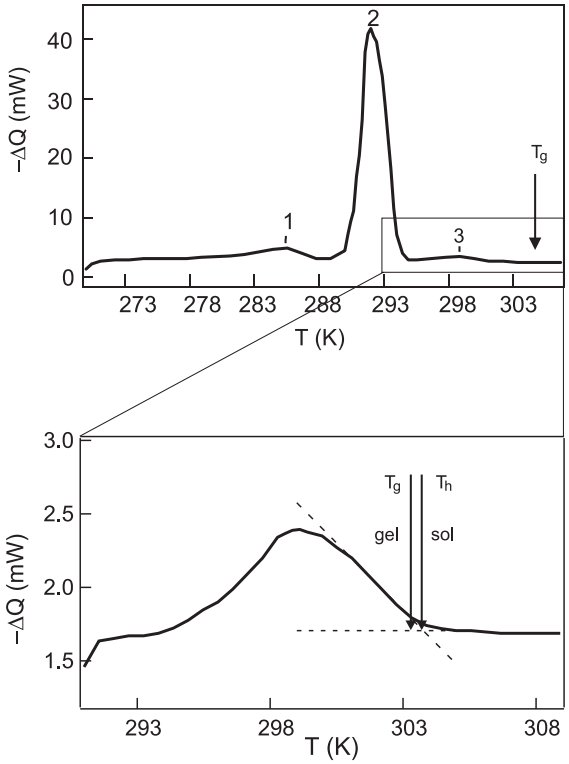

Figure 2. Calorimetric measurements of the 28.9% dispersions of sample 1 in n-hexadecane, starting at 268 K (top) and 291 K (bottom). The heating rate in both cases was +0.5 K min^{-1}. T_g denotes the cloud-point temperature, while T_h marks the high-temperature onset. There was no observed hysteresis in the measurements.

1 in n-hexadecane at $\varphi \approx 5\%$. In the dispersions of sample 3 gel formation in n-hexadecane-d_{34} occurred at $\varphi \approx 6\%$. However, for sample 1 in toluene gel formation was not observed until $\varphi \approx 31\%$ and not any more around 10%. The dispersion of sample 3 in benzene-d_6 showed gelation at volume fractions of approximately 22%. Combining our observations with those of [9, 18] it seems clear that dispersions of stearyl-coated silica particles in n-hexadecane (and other longer n-alkanes) have a stronger tendency to gel formation than dispersions in toluene, benzene or CCl_4.

In order to clarify this difference we have performed calorimetric measurements on three stearyl-coated silica particles in n-hexadecane and for comparison also a measurement in toluene. A typical measurement of a dispersion in n-hexadecane is given in figure 2, showing three peaks.

The first two peaks (marked 1 and 2 at lower temperature), also present in the pure solvent are related to the n-hexadecane itself (peak 2 is the melting peak of n-hexadecane) and are not relevant for the present study. The third peak only appears in the n-hexadecane dispersion at a temperature that nearly coincides with the gel formation temperature. The bottom panel shows a calorimetric measurement over a shorter temperature range of temperatures, starting right above the melting point of n-hexadecane (291 K). By integrating the peak we find (for this particular measurement) that 4.8 J is absorbed per gram dispersion. The results for all dispersions are collected in table 2, giving the temperature of the peak maximum (T_{max}), the

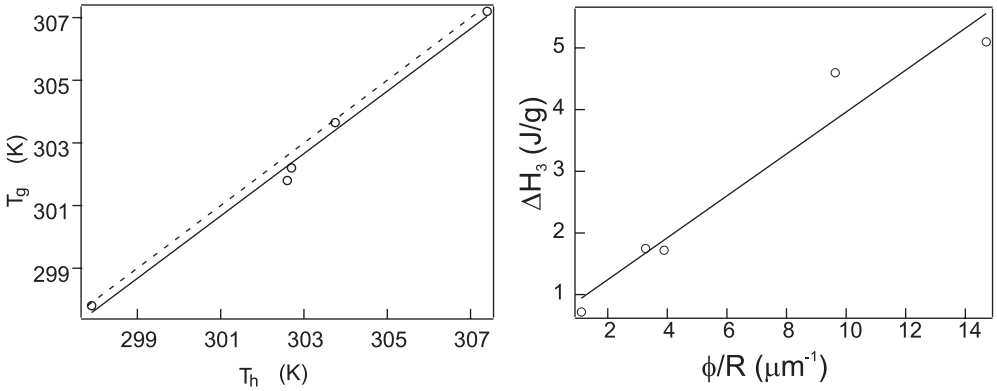

Figure 3. Left: plot of gelation temperature (T_g) against the onset of the heat uptake (T_h). The solid line is a linear fit. The dashed line marks $T_g = T_h$. Right: plot of ΔH_3 against φ/R_{TEM} as a measure of the total particle surface area. The straight line shows a proportionality relation.

Table 2. Calorimetry and cloud-point results for dispersions in n-hexadecane and toluene.

Particles	φ (v/v%)	T_{max} (K)	T_h (K)	ΔH_3 (J g^{-1})	T_g (K)
			$C_{16}H_{34}$		
Sample 1	3.35	298.4	302.6	0.72[a]	301.8[d]
Sample 1	9.80	298.8	302.7	1.75[a]	302.6[d]/301.6[e]
Sample 1	28.9	298.9	303.8	5.0[a,c]/4.2[b]	303.7[d]/303.6[e]
Sample 2	28.4	295.3	297.9	1.72[b]	297.8[e]
Sample 4	29.4	302.0	307.4	5.1[b]	307.2[d]
			C_7H_8		
Sample 1	28.9	—	—	<0.5	280.9

[a] Scan speed 0.2 K min^{-1}.
[b] Scan speed 0.5 K min^{-1}.
[c] Two runs after 3 days' storage first gave 5.2 and then 4.8 J g^{-1}.
[d] Bending point in a turbidity–temperature scan.
[e] Lowest temperature at which the dispersion flows.

extrapolated temperature as a measure of the high-temperature starting point of the peak (T_h, see figure 2), the integrated transition enthalpy (ΔH_3) and the temperature of the transition in the dispersion (T_g).

In the left panel of figure 3 we have plotted T_g against T_h for all dispersions that exhibit gelation. This shows that there is a clear correlation between gelation and heat production and that (with increasing temperature) heat absorption precedes gel breakup. The right panel shows the integrated transition enthalpy as a function of surface area (φ/R_{TEM}, which is proportional to the total surface area). The observed proportionality indicates that the observed heat effect is related to transition at the particle interfaces. The remaining deviations from a proportional relation might be attributed to experimental errors, variations in the stearyl coating density, variations in the roughness of the surface on the length scale of the stearyl chain, and to inaccuracies in the estimate of the total surface area, e.g. because the particle shape is not perfectly spherical and because of variations in the size distribution of the particles [6].

As the heat uptake associated with the gelation transition is present in n-hexadecane dispersions but absent in toluene, it is evident from the above measurements that the solvent

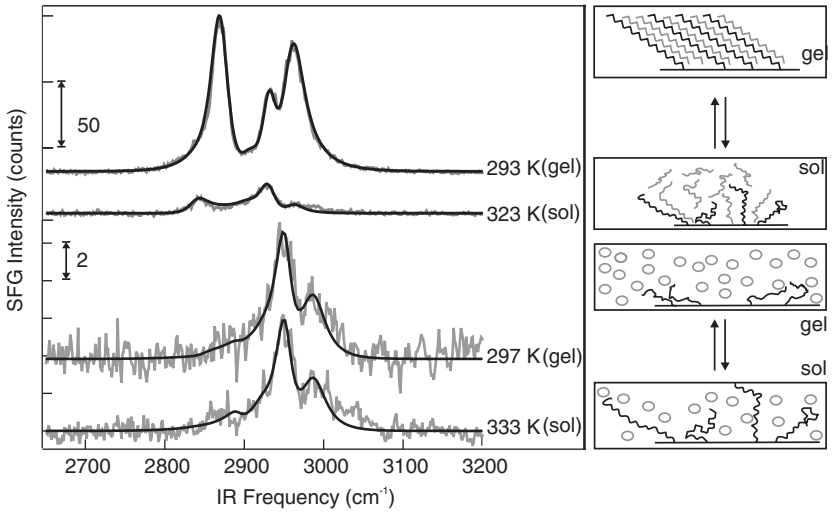

Figure 4. SFG scattering spectra (grey lines) of a dispersion of silica particles (sample 3) in n-hexadecane in gel and sol state (top two spectra) and dispersions in benzene in gel and sol state (bottom two spectra). The difference in signal to noise is due to the difference in refractive index of the benzene and n-hexadecane solvents.

plays an important role in the energetics of the gelation transition. This is further corroborated by the fact that no heat effect was observed when the calorimetry measurements were performed on dried samples. These results are in agreement with published results on calorimetric measurements on stearyl silica particles in the dry state as well as dispersed in toluene [10], where only a broad transition was observed. Indeed, we did not find a sharp transition as observed in the n-hexadecane dispersions. Also calorimetric measurements on dry octadecyl-coated silica as used in chromatography columns gave similar results [8].

3.2. Vibrational sum frequency scattering

From the above description it is very likely that the interaction of the interface with the solvent plays a crucial role in the difference in gelation behaviour. To investigate the role of the surface–solvent interaction on a molecular level we have recorded and compared SFG scattering spectra of gels and sols of 24 vol% dispersions of sample 3 particles in different solvents. Figure 4 shows SFG spectra of dispersions in n-hexadecane-d_{34} and benzene-d_6 at two different temperatures for which both samples are in different states as indicated in the graph.

The scattered sum frequency field can be described very well with the well-known expressions for SFG, where the local surface susceptibility ($\chi^{(2)}$) has been replaced by an effective particle susceptibility ($\Gamma^{(2)}$), which has to be convoluted with the spectrum of the upconversion field (E_{VIS}) [24, 25]:

$$I_{\mathrm{SFG}}(\omega) \propto \left| \sum_n \int_{-\infty}^{\infty} \Gamma_n^{(2)}(\omega') E_{\mathrm{VIS}}(\omega' - \omega)\, \mathrm{d}\omega' \right|^2, \qquad \Gamma_n^{(2)}(\omega) = \frac{\mathrm{A}_n}{(\omega - \omega_{0\mathrm{n}}) + \mathrm{i}\Upsilon_{\mathrm{n}}} \tag{1}$$

where n refers to a vibrational mode with resonance frequency $\omega_{0\mathrm{n}}$ and spectral half width at half maximum, Υ_{n}. The solid lines in figure 4 are fits to the data using this equation. The fits were obtained with the resonance frequencies for the well-known symmetric CH_2 and CH_3 stretching modes (at 2854 and 2889 cm^{-1} respectively), the asymmetric CH_3 stretch vibration

(2978 cm^{-1}), the Fermi resonances of the symmetric CH_3 stretching mode with an overtone of the CH_3 bending mode (2953 cm^{-1}) and a Fermi resonance of the asymmetric CH_2 stretching mode with in-plane methylene (CH_2) deformations (2925 cm^{-1}) [31, 32].

As already discussed in [26], the dramatic changes in the spectra of the dispersion in n-hexadecane reflect the appearance of an ordered layer (at lower temperatures) of surface molecules in which all molecules are collectively tilted away from the local surface normal with an angle of 52°. The surface order–disorder transition (depicted in figure 4) occurs at temperatures below the cloud-point and coincides with the temperatures at which the heat effect occurs.

In contrast to the dramatic changes observed in n-hexadecane, figure 4 shows that there is little change in the SFG signal following the gelation transition in benzene. The same observations were made for dispersions in CCl_4. These spectra clearly lack the intense signal at the frequency of the symmetric CH_3 vibrational mode, which generally indicates an ordered layer [33, 34]. At temperatures both above and below the gelation temperature, the surface layer is disordered. Thus, dispersions in benzene and CCl_4 do not display a surface order–disorder transition. This does not necessarily mean that the surface layer has the same structure at both temperatures. As a function of temperature the density of the solvent changes more rapidly than that of the silica particles. As a consequence, the refractive index mismatch increases with lower temperatures. One can expect a denser surface layer (accompanied by a stronger van der Waals interaction) at lower temperatures for benzene, leading to a somewhat different surface structure.

Having observed the difference on the molecular level as well as on the macroscopic level, we can explain the difference in gelation behaviour for different solvents. A gelation transition can occur as a function of temperature if the interaction potential changes at lower temperatures such that the particle–particle interaction becomes attractive. This can happen due to changing densities of solvent and particles. This effect occurs for all solvents and particles. However, if the solvent can interdigitate with the surface chains on the particles, the free energy can be reduced even further (at lower temperatures) by forming an ordered layer. In the case of benzene and CCl_4, such an ordered layer cannot be formed. As a consequence a surface transition (that liberates a lot of heat) cannot take place. Both cases are illustrated in the right panel of figure 4. In the case of n-hexadecane (and probably for all long-chain n-alkanes), such an ordered layer can be formed. The measured heat that is produced varies from 4.8 to 5.2 J g^{-1} for the most concentrated gel of particles of sample 1. Given that the heat of fusion of our n-hexadecane is 228.8 J g^{-1} and using $\sigma_{TEM} = 30$ nm and a dispersion density of 1.057 g ml^{-1}, the observed 4.8 J g^{-1} corresponds to melting of a surface layer of n-hexadecane with a thickness of 1.1 nm. The production of this amount of heat, together with the changes in the sum frequency scattering spectra, clearly suggests the formation of a crystalline layer. Because the transition occurs only a few degrees above the melting temperature of n-hexadecane (291 K), this behaviour can be associated to the surface melting phenomenon that has been observed in a series of alkanes a few degrees above their melting point [35].

4. Surface layer in n-hexadecane

To investigate whether the order is confined to the first layer we have also taken SFG spectra of a 24 vol% gel in a 4:1 mixture of n-hexadecane-d_{34} with n-hexadecane as solvent. Replacing part of the deuterated solvent by non-deuterated solvent does not affect the phase behaviour of the dispersion (see [36]).

The SFG spectrum of an ordered layer is dominated by the vibrations of the methyl (CH_3) groups. Also, as part of the solvent is non-deuterated some of the signal might be lost due to

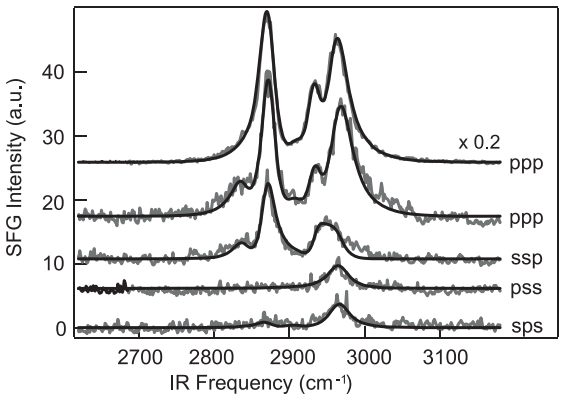

Figure 5. SFG spectra (grey lines) obtained at different polarization conditions of a gel of colloidal particles (sample 3) in 20/80 vol% n-hexadecane/n-hexadecane-d_{34}. The spectra were taken at polarization combinations ppp, ssp, pss and sps and collected at a scattering angle of 51°. The black lines are fits as described in the text. The top trace shows the SFG spectra of a gel with fully deuterated n-hexadecane in ppp polarization combination (the same as in figure 4).

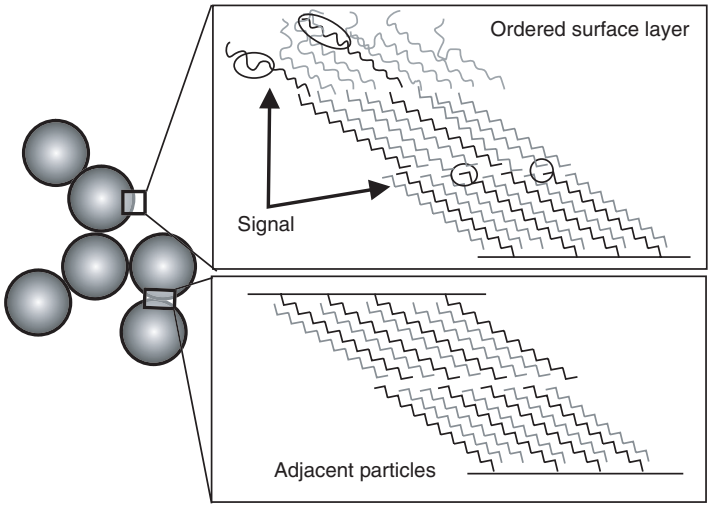

Figure 6. Illustration of two important structures related to gelation in n-hexadecane. The black chains represent C–H chains (that are resonantly excited by the infrared field and thus contribute to the SFG signal) whereas the grey chains represent C–D chains (that are not excited and do not contribute to the scattered signal). Due to the vector nature of the created polarization, a pair of oppositely oriented dipoles will not generate a net sum frequency field. As a result, only the encircled molecular groups (in the upper panel) will contribute to the signal. There will be no sum frequency scattering from particle regions that have a geometry that resembles the one sketched in the lower panel.

destructive interference with methyl (CH_3) groups that are pointing in the opposite direction. The amount of intensity loss critically depends on the structure of the layer. If local inversion symmetry exists over a long range around the particle, a large portion of the signal might be lost. This is illustrated in figure 6, in which two adjacent particles are sketched. A disordered layer on the other hand can be expected to be dominated by the methyl (CH_2) stretching modes and the Fermi resonances. Figure 5 shows SFG spectra taken at different polarization combinations

of a 24 vol% gel in a 4:1 mixture of n-hexadecane-d_{34} and n-hexadecane as solvent. These spectra are fitted with the same parameters as used in the fits of figure 4, and from the fits the same average tilt angle of $52° \pm 5°$ can be obtained [26]. These gel spectra are dominated by the methyl (CH_3) stretching modes, but there is also a clear signal from the symmetric methylene (CH_2) stretching mode (at $\sim$2854 cm^{-1}). Also, it can be seen that the signal from the gel state in a solvent mixture is over a factor of 5 smaller than the signal from the gel in 100% n-hexadecane-d_{34}. This dramatic decrease in intensity is much more than expected if we take the absorption of the infrared field by the non-deuterated solvent into account (which amounts to a intensity loss of 15%).

As mentioned, both the decrease in intensity as well as the appearance of CH_2 resonances are related to the structure of the solvent around the particles. The loss of intensity cannot be due to disorder as witnessed by the strong signal from the methyl (CH_3) groups (compared to that of the methylene (CH_2) groups), that still dominate the spectrum. The CH_2 resonances should be much stronger than what is observed, if disorder were to be responsible for the decrease in the overall signal (see e.g. [34]). As mentioned above, the alkyl chains are not densely packed on the surface, and to form a crystalline layer the solvent molecules must participate to form an ordered layer. The dramatic intensity difference upon partially non-deuterating can be explained by the formation of one (or several) more or less ordered layers on top of the first, leading to partial restoration of local inversion symmetry as sketched in figure 6. It explains why a relatively small amount of non-deuterated solvent leads to a disproportionate change in intensity. The ordered layers gradually transform into disordered solvent, which leads to the appearance of more pronounced methyl (CH_2) stretch modes that are representative of the number of chain defects.

Assuming a simple model of a single ordered interface layer with one or more ordered shells on top that terminates in one layer (as sketched in figure 6), we can estimate the fraction of stearyl chains in the crystalline film by simply comparing the amplitudes of the scattered signal with fully deuterated and partially deuterated solvent. The scattered amplitude is directly proportional to the number of CH_3 groups that contribute to the signal. In the case of fully deuterated solvent, 100% of the stearyl chains account for the signal. In the case of partially deuterated solvent, only the non-deuterated solvent molecules that have one ordered head group and one randomly oriented head group can cause destructive interference that leads to a decrease in amplitude. The amplitude decrease can be determined from the spectral fits, which amounts to a factor of 0.38. (The fully ordered solvent molecules do not contribute, since both CH_3 groups are oriented in opposite directions and thus the corresponding dipole moments cancel each other out.) Since we know the volume fraction of the signal-cancelling molecules (20%), we can retrace the fraction of stearyl chains that are chemically linked to the surface silanol groups. This results in a volume fraction of 0.32 ± 0.05, which corresponds to a surface area of 1.03 nm^2 per stearyl chain. This procedure is of course only valid to the extent that the particle shape is spherical and smooth and that they are monodisperse. From table 1 we can check the latter. From TEM analysis [24] we found a spherical form factor of 1.04 (the actual average area compared to the spherical area using the particle radius) which justifies our assumptions.

This area is much higher than the ones found from elemental analysis, in which areas as low as 0.21 nm^2 per stearyl chain were reported [6, 37]. However, these particles are relatively small (up to a radius of $\sim$50 nm) and it was reported that the surfaces might very well exhibit roughness on a small scale, leading to a larger total surface area.

Thus, by comparing scattering measurements in partially deuterated solvent with those in fully deuterated solvent we are able to deduce that loss of order is gradual. This kind of gradual loss in order has also been observed for multilayered self-assembled monolayers

(SAMs) of stearic acid [38] and compares favourably to previous studies on surface freezing in n-alkanes [35, 39].

5. Conclusions

Gelation of stearyl-coated silica particles occurs at lower volume fractions in n-hexadecane solvent compared to solvents like toluene, benzene and CCl_4. In n-hexadecane it is associated with an anomalous heat effect, that is absent for the other solvents. Comparing heat uptake with available surface area clearly indicates that the interface plays a key role in the observed effect. Vibrational sum frequency scattering experiments are sensitive to the molecular structure of the particle–solvent interface and reveal that indeed the heat effect can be associated to a molecular order–disorder transition. This can only occur if the solvent can interdigitate with the surface crafted layer. We find that the loss of order in such a layer occurs gradually.

Acknowledgments

The authors would like to thank R C V van Schie and P Schakel for excellent technical support, and A W Kleyn, J E G J Wijnhoven, A V Petukhov and H N W Lekkerkerker for many helpful discussions. SR acknowledges support form the Alexander von Humboldt foundation. This work is part of the research program of the Foundation for Fundamental Research on Matter (FOM), which is financially supported by the Netherlands Organization for Scientific Research (NWO).

References

[1] Baksh M M, Jaros M and Groves J T 2004 *Nature* **427** 139
[2] Anderson V J and Lekkerkerker H N W 2002 *Nature* **416** 811
[3] Taton T A, Mirkin C A and Letsinger R L 2000 *Science* **289** 1757
[4] Lukatsky D B and Frenkel D 2004 *Phys. Rev. Lett.* **92** 068302
[5] Frenkel D 2002 *Physica* A **313** 1
[6] van Helden A K, Jansen J W and Vrij A 1981 *J. Colloid Interface Sci.* **81** 354
[7] Jansen J W, de Kruif C G and Vrij A 1984 *Chem. Phys. Lett.* **107** 450
[8] van Miltenburg J C and Hammers W E 1983 *J. Chromatogr.* **268** 147
[9] Jansen J W, de Kruif C G and Vrij A 1986 *J. Colloid Interface Sci.* **114** 481
[10] de Kruif C G and van Miltenburg J C 1990 *J. Chem. Phys.* **93** 6865
[11] Rouw P W and de Kruif C G 1988 *J. Chem. Phys.* **88** 7799
[12] Rouw P W, Woutersen A T J M, Ackerson B J and de Kruif C G 1989 *Physica* A **156** 876
[13] Rouw P W and de Kruif C G 1989 *Phys. Rev.* A **39** 5399
[14] Solomon M J and Varadan P 2001 *Phys. Rev.* E **63** 051402
[15] de Kruif C G and Schouten J A 1990 *J. Chem. Phys.* **92** 6098
[16] Chen M and Russel W B 1991 *J. Colloid Interface Sci.* **141** 564
[17] Bergenhotz J and Fuchs M 1999 *J. Phys.: Condens. Matter* **11** 10171
[18] Grant M C and Russel W B 1993 *Phys. Rev.* E **47** 2606
[19] Wang H, Yan E C Y, Borguet E and Eisenthal K B 1996 *Chem. Phys. Lett.* **259** 15
[20] Wang H, Yan E C Y, Liu Y and Eisenthal K B 1998 *J. Phys. Chem.* B **102** 4446
[21] Ma G and Allen H C 2001 *J. Am. Chem. Soc.* **124** 9374
[22] Dadap J I, Shan J, Eisenthal K B and Heinz T F 1999 *Phys. Rev. Lett.* **83** 4045
[23] Yang N, Angerer W E and Yodh A G 2001 *Phys. Rev. Lett.* **87** 103902
[24] Roke S, Roeterdink W G, Wijnhoven J E G J, Petukhov A V, Kleyn A W and Bonn M 2003 *Phys. Rev. Lett.* **91** 258302
[25] Roke S, Bonn M and Petukhov A V 2004 *Phys. Rev.* B **70** 115106
[26] Roke S, Buitenhuis J, van Blaaderen A and Bonn M 2005 submitted
[27] Stöber W, Fink A and Bohn E 1968 *J. Colloid Interface Sci.* **26** 62

[28] Coenen S and de Kruif C 1988 *J. Colloid Interface Sci.* **124** 104
[29] van der Ham E W M, Vrehen Q H F and Eliel E R 1996 *Surf. Sci.* **386** 96
[30] Richter L J, Petralli-Mallow T P and Stephenson J C 1998 *Opt. Lett.* **23** 1594
[31] Zhuang X, Miranda P B, Kim D and Shen Y R 1999 *Phys. Rev.* B **59** 12632
[32] Bell G R, Bain C D and Ward R N 1996 *J. Chem. Soc. Faraday* **92** 515
[33] Guyot-Sionnest P, Hunt J H and Shen Y R 1987 *Phys. Rev. Lett.* **59** 1597
[34] Roke S, Schins J M, Müller M and Bonn M 2003 *Phys. Rev. Lett.* **90** 128101
[35] Ocko B M, Wu X Z, Sirota E B, Sinha S K, Gang O and Deutsch M 1997 *Phys. Rev.* E **55** 3164
[36] Dorset D L, Strauss H L and Snyder R G 1991 *J. Phys. Chem.* **95** 938
[37] Ballard C C, Broge E C, McWhorther J R, Iler R K and John D S S 1961 *J. Phys. Chem.* **65** 20
[38] Ye S, Noda H, Morita S, Uosaki K and Osawa M 2003 *Langmuir* **19** 2238
[39] Sloutskin E, Wu X Z, Peterson T B, Gang O, Ocko B M, Sirota E B and Deutsch M 2003 *Phys. Rev.* E **68** 031605